OFFICE OF NAVAL RESEARCH

Contract N00014-87-K-0531

R & T Code 431a016

TECHNICAL REPORT NO. 4

Solid-State Phase Equilibria in the ZnS-Ga_2S_3 System

by

J.M. Zhang, W.W. Chen, A.J. Ardell and B. Dunn

Prepared for Publication in

JOURNAL OF THE AMERICAN CERAMIC SOCIETY

Department of Materials Science and Engineering
University of California, Los Angeles,
Los Angeles, California 90024

October 1, 1989

SECURITY CLASSIFICATION OF THIS PAGE

REPORT DOCUMENTATION PAGE

1a. REPORT SECURITY CLASSIFICATION Unclassified	1b. RESTRICTIVE MARKINGS
2a. SECURITY CLASSIFICATION AUTHORITY	3. DISTRIBUTION / AVAILABILITY OF REPORT Approved for public release: Distribution Unlimited
2b. DECLASSIFICATION / DOWNGRADING SCHEDULE	
4. PERFORMING ORGANIZATION REPORT NUMBER(S) No. 4	5. MONITORING ORGANIZATION REPORT NUMBER(S) N00014-87-K-0531
6a. NAME OF PERFORMING ORGANIZATION University of California Los Angeles/Bruce Dunn 6b. OFFICE SYMBOL (If applicable)	7a. NAME OF MONITORING ORGANIZATION Office of Naval Research Dr. R. Schwartz
6c. ADDRESS (City, State, and ZIP Code) Department of Materials Science & Engineering University of California, Los Angeles, 90024-1595	7b. ADDRESS (City, State, and ZIP Code) Code 38504 Naval Weapons Center China Lake, CA 93555
8a. NAME OF FUNDING / SPONSORING ORGANIZATION 8b. OFFICE SYMBOL (If applicable)	9. PROCUREMENT INSTRUMENT IDENTIFICATION NUMBER
8c. ADDRESS (City, State, and ZIP Code)	10. SOURCE OF FUNDING NUMBERS PROGRAM ELEMENT NO. / PROJECT NO. / TASK NO. / WORK UNIT NO.

11. TITLE (Include Security Classification)
Solid-State Phase Equilibria in the ZnS - Ga_2S_3 System

12. PERSONAL AUTHOR(S)
J. M. Zhang, W. W. Chen, A. J. Ardell and B. Dunn

13a. TYPE OF REPORT	13b. TIME COVERED	14. DATE OF REPORT (Year, Month, Day)	15. PAGE COUNT
Technical	FROM 9/88 TO 9/88	1989, October 1	18

16. SUPPLEMENTARY NOTATION
Submitted for publication in Journal of the American Ceramic Society

17. COSATI CODES			18. SUBJECT TERMS (Continue on reverse if necessary and identify by block number)
FIELD	GROUP	SUB-GROUP	

19. ABSTRACT (Continue on reverse if necessary and identify by block number)

ABSTRACT

The ZnS-Ga_2S_3 equilibrium phase diagram has been determined to 50 mol % over the temperature range 700 to 900 ° C. Samples of various compositions were prepared via solid-state diffusion starting from powders of the pure components. The identification of the phases was determined by x-ray diffraction methods. The principal feature of the phase equilibria is the eutectoid transformation at 818 ° hexagonal wurtzite containing ~ 16 mol % Ga_2S_3 to cubic ZnS and tetragonal $ZnGa_2S_4$. $ZnGa_2S_4$ is the equilibrium compund at 50 mol % Ga_2S_3, but it exists over a considerable range of stoichiometry. The solubility of Ga_2S_3 in ZnS increases with increasing temperature to a maximum of ~ 9 mol% at the eutectoid temperature.

20. DISTRIBUTION / AVAILABILITY OF ABSTRACT ☐ UNCLASSIFIED/UNLIMITED ☐ SAME AS RPT. ☐ DTIC USERS	21. ABSTRACT SECURITY CLASSIFICATION
22a. NAME OF RESPONSIBLE INDIVIDUAL	22b. TELEPHONE (Include Area Code) / 22c. OFFICE SYMBOL

DD FORM 1473, 84 MAR — 83 APR edition may be used until exhausted. All other editions are obsolete.

SECURITY CLASSIFICATION OF THIS PAGE

SOLID STATE PHASE EQUILIBRIA IN THE ZnS-Ga_2S_3 SYSTEM

Jimin M. Zhang, William W. Chen, Alan J. Ardell and Bruce Dunn*

Department of Materials Science and Engineering

University of California

Los Angeles, CA 90024

August 1989

Key Words: phase diagram, ZnS, Ga_2S_3, $ZnGa_2S_4$, eutectoid reaction

*Member, American Ceramic Society

ABSTRACT

The ZnS-Ga_2S_3 equilibrium phase diagram has been determined to 50 mol % over the temperature range 700 to 900 °C. Samples of various compositions were prepared via solid-state diffusion starting from powders of the pure components. The identification of the phases was determined by x-ray diffraction methods. The principal feature of the phase equilibria is the eutectoid transformation at 818 °C of hexagonal wurtzite containing ~16 mol %Ga_2S_3 to cubic ZnS and tetragonal $ZnGa_2S_4$. $ZnGa_2S_4$ is the equilibrium compound at 50 mol %Ga_2S_3, but it exists over a considerable range of stoichiometry. The solubility of Ga_2S_3 in ZnS increases with increasing temperature to a maximum of ~9 mol% at the eutectoid temperature.

INTRODUCTION

ZnS is commercially used as an infrared (IR) transmitting material because of its good optical transmission up to 12 μm and adequate mechanical strength. However, ceramics with improved fracture toughness, thermal-shock resistance and erosion resistance are absolutely essential for certain IR-window applications. There are several possible approaches to the engineering of ceramics with this combination of improved mechanical properties while retaining infrared transmittance comparable to that of ZnS. Our approach is to explore the possibilities of strengthening and toughening ZnS by the addition of dispersions of particles of a second-phase, with the dispersoids introduced into the microstructure by the appropriate heat-treatment of densified samples.

The controlled introduction of second-phase precipitates into a material by heat-treatment is a well-established procedure for strengthening and toughening of metallurgical alloys. High-strength commercial aluminum alloys through precipitation hardening, and tough steels produced by tempering are especially well-known examples. In ceramic materials, precipitation hardening has been investigated in MgO single crystals containing $MgFe_2O_4$ (spinel) precipitates[1], while significant toughening has been demonstrated in two-phase ceramics such as monocrystalline LiF containing large MgF_2 particles[2] and various ZrO_2-containing ceramic alloys[3].

We are currently attempting to increase the strength and toughness of ZnS ceramics through the addition of second-phase constituents, where the second phase particles are introduced by heat treatment. In the specific

case of ZnS the second-phase additions should have intrinsically good IR transmittance and a closely matching refractive index in order to minimize optical attenuation losses due to scattering. This requirement places certain restrictions on the suitability of the ions added for alloying purposes.

Clearly, to explore the objective of improving the mechanical behavior of ZnS through heat treatment, knowledge of solid-solid phase equilibria involving ZnS and other sulfides is essential. Unfortunately, such data are limited, and we have had to undertake the task of determining some binary phase diagrams ourselves. Among the various possibilities we have considered, the ZnS-CdS and ZnS-Ga_2S_3 systems appear to be especially promising for meeting all the requirements noted above. We have already reported the results of the determination of the ZnS-rich portion of the ZnS-CdS phase diagram[4], and have presented a preliminary version of the ZnS-Ga_2S_3 phase diagram[5]. In this paper, we present the ZnS-Ga_2S_3 phase diagram to 50 mol% Ga_2S_3, at the same time refining the earlier version.

The first study of this phase diagram was made by Gates and Edwards[6], using the simultaneous Knudson and dynamic torsion-effusion method. They published the Ga_2S_3-rich end of the partial ZnS-Ga_2S_3 phase diagram, locating the phase boundaries to within ±15 °C. However, this part of the diagram is of no interest for strengthening ZnS-based ceramics. Malevskii[7] studied the ZnS-Ga_2S_3 system using the solid-state reaction technique and published a partial phase diagram at the ZnS-rich end. His work has established that the solubility of Ga_2S_3 increases with increasing temperature, and that the diagram contains a eutectoid reaction around 800 °C. The eutectoid reaction is such that wurtzite containing between 15

and 20 mol % Ga_2S_3 decomposes to form sphalerite and the thiogallate phase $ZnGa_2S_4$.

$ZnGa_2S_4$ itself is a good IR-transmitting material in the range 2.5 to 12 μm and has the $I\bar{4}2m$ tetragonal crystal structure[8,9]. The tetragonal unit cell has lattice parameters, a_t and c_t of 0.5297 and 1.0363 nm respectively[9]. The lattice mismatch with cubic sphalerite ZnS (a_c = 0.5410 nm) is very small, which probably accounts for the fairly large solubility of thiogallate in sphalerite (despite the difference in valence between Zn and Ga) reported by Malevskii. Also, the microhardness of $ZnGa_2S_4$ has been found to be close in value to that of ZnS[10].

Based on the factors discussed above, it is clear that Ga_2S_3 satisfies the requirements for a suitable second phase addition. ZnS-rich solid solutions should be precipitation hardenable, whereas alloys of near eutectoid composition offer the prospect of microstructural manipulation by eutectoid decomposition. Additionally, the expected decomposition product, $ZnGa_2S_4$, is optically compatible with ZnS. The major drawback to the development of these "alloys" as IR materials is the accuracy of Malevskii's phase diagram, because the compositions of the samples used in his investigation differed by as much as 10 mol%. This was the main reason for undertaking the current investigation.

EXPERIMENTAL

X-ray diffraction was the principal technique employed to investigate the phase equilibria. Powders of ZnS (99.9%, Aesar) and Ga_2S_3 (99.99%, Alfa) were used as starting materials for the preparation of alloys by solid-state reaction. The method of preparation used in the present study was

previously described by Chen et al.[4] The powders were mixed, ground with a mortar and pestle, sealed under vacuum in a fused silica ampoule and heated to the reaction temperature. In order to assure that equilibrium was attained, a solid-state sintering period of more than 10 weeks was used at 700 °C, but shorter times were used at the higher reaction temperatures. The various conditions are summarized in Table I. The intervals in composition of the samples were 1 or 2 mol% near the phase boundaries and 3 or 5 mol% elsewhere. We have found that the approach to equilibrium is far faster for the mixed powders than for compacted samples of identical composition. This is because the eutectoid decomposition reaction is very sluggish.

The parametric method[11] and a modified version of the disappearing-phase method[11,12] were used to establish the solvus compositions. The choice of method was determined by the crystal structures of the equilibrium phases present. In particular, the x-ray diffraction peaks of wurtzite are readily distinguished from those of the sphalerite and thiogallate phases. However, the sphalerite and thiogallate phases are structurally similar, and many of their peaks overlap. For this reason, the disappearing phase method was used to determine the phase boundaries at 850 and 900 °C, where wurtzite is in equilibrium with either sphalerite or thiogallate, depending on composition. The parametric method was used to establish the phase boundaries between the low-temperature sphalerite and thiogallate phases.

The parametric method takes advantage of the variation of the lattice constants with solute concentration in solid solutions. It is a classical technique which is thoroughly described by Cullity[11], and requires no fur-

ther discussion except to note that NaCl powder (99.98%, Fisher) was mixed with the reacted samples for use as an internal standard in the x-ray diffraction analysis. Ni-filtered Cu Kα x-rays were employed, with the diffractometer operating in a digital step-scanning mode (0.01° for 10 or 20 s).

The basis of the disappearing phase method is that the fraction of a particular phase present in the alloy is proportional to the integrated intensity, I, of one of its x-ray peaks. Klug and Alexander[12] have shown that in a two-phase mixture of, say, the wurtzite (w) and thiogallate (t) phases, the x-ray intensity of wurtzite can be expressed as

$$\frac{I_w}{I_{wp}} = \frac{X_w\mu_w}{X_w(\mu_w-\mu_t) + \mu_t} = \frac{X_w\mu_w}{X_w\mu_w + X_t\mu_t} \qquad (1)$$

where I_w is the intensity of a specific wurtzite peak in the two-phase mixture, I_{wp} is the intensity of the same peak, but when the material is 100 % wurtzite containing its equilibrium concentration of Ga_2S_3 (this is *not* pure wurtzite), the μ's are mass absorption coefficients of the two phases at their equilibrium concentrations of Ga_2S_3, and the X's are the fractions by weight of the two phases.

Equation (1) is not in an especially useful form because I_{wp} is difficult to measure (measurement of I_{wp} requires the preparation of wurtzite containing its equilibrium concentration of Ga_2S_3 at a particular temperature, which is precisely what we are trying to determine). To transform it into a useful equation, we first write it as

$$\frac{I_w}{I_w + I_t} = \frac{I_{wp}X_w\mu_w}{I_{wp}X_w\mu_w + I_{tp}X_t\mu_t}, \qquad (2)$$

which makes use of the counterpart of equation (1) written for the thiogallate phase instead. We then apply the lever rule, i. e.

$$X_w = \frac{W_o - W_w}{W_t - W_w} ; X_t = \frac{W_t - W_o}{W_t - W_w},$$

where W_o is the weight fraction of Ga_2S_3 in the sample, and W_w and W_t are the equilibrium weight fractions of Ga_2S_3 in the wurtzite and thiogallate phases, respectively. Substitution of these into equation (2) produces the result

$$\frac{I_w}{I_w + I_t} = \frac{W_o - W_w}{W_o - W_w + \frac{I_{tp}\mu_t}{I_{wp}\mu_w}(W_t - W_o)}. \quad (3)$$

Since the ratio $I_{tp}\mu_t/I_{wp}\mu_w$ is constant within the two-phase W + T region at any specific temperature, and $W_w < W_o < W_t$, the ratio $I_w/(I_w + I_t)$ clearly varies between 0 and 1 as the equilibrium solvus compositions are approached. If $I_{tp}\mu_t/I_{wp}\mu_w$ were equal to unity the variation of $I_w/(I_w + I_t)$ with W_o would be linear. Such is not generally the case, however, which introduces curvature into such plots even if the diffraction peaks chosen are nearly equally intense when the relative proportions of the two phases are approximately equal (i. e., when $X_w \approx X_t \approx 0.5$).

In the application of equation (3) to our experimental data, the {331} sphalerite peak, the {0002} {20$\bar{2}$3} {21$\bar{3}$0} and {21$\bar{3}$1} wurtzite peaks, and the {112} {316} and {413} thiogallate peaks were used for the intensity measurements. The integrated intensities were calculated using the POW computer program[13]. This program subtracts the $K\alpha_2$ component and calculates the integrated intensities with a relative error of less than 2%.

RESULTS AND DISCUSSION

Phase Fields in the ZnS-$ZnGa_2S_4$ Pseudobinary System

An analysis of the diffraction peaks identified the phases present in the sample. The results are plotted in Fig. 1, where the shaded regions indicate the positions of the phase boundaries consistent with the data. Preliminary examination revealed the existence of three different solid solution phases, namely sphalerite (S), wurtzite (W) and the tetragonal thiogallate (T) and three two-phase fields (S + W, S + T, W + T). It is obvious that the wurtzite solid solution must undergo the eutectoid transformation W $\rightarrow$ S + T, but the eutectoid temperature and composition cannot be determined accurately from the information in Fig. 1. All of these general features were noted by Malevskii[7], although his diagram is in disagreement with the data in Fig. 1.

Quantitative Evaluation of the Phase Boundaries

Figure 2 shows examples of the use of the disappearing phase method used to determine the S/W and W/T solvi at two different temperatures. The intensity ratios $I_s/(I_s + I_w)$ and $I_w/(I_w + I_t)$ are plotted for the S + W and W + T phase fields, respectively. The data were fitted by a fourth-order polynomial for purposes of extrapolation to 0 and 100 % of the phases present, and the intersections were taken as the equilibrium compositions. The use of a high-order polynomial obviated the need to impose any assumptions on the behavior of the intensity ratios with composition, and illustrates the non-linear nature of equation (3).

At 800 °C and below, the two-phase region consists only of sphalerite and thiogallate, and, as already noted, the parametric method is more accurate in this temperature range. Examples of its use are shown in Fig. 3. For the ZnS-rich end, the lattice constant of sphalerite, **a**, is plotted *vs* mol % Ga_2S_3 using the angular position of the {331} sphalerite peak to calculate **a**. The solvus compositions at 700 and 750°C are located at 5.1 and 6 mol% Ga_2S_3. At the $ZnGa_2S_4$-rich end, the positions of the {400}, {316} and {413} peaks were used to calculate $\mathbf{a}_t$ as a function of the mol % Ga_2S_3. The boundary between the one and two-phase region is 44 % Ga_2S_3 at 700 and 41% at 800 °C.

The ZnS-Ga_2S_3 phase diagram thus obtained from a combination of the two methods is shown in Fig. 4. Extrapolation of the phase boundaries between the one and two-phase fields was used to determine the eutectoid composition and temperature, which were assumed to be the point of intersection of the high-temperature data. Since the data at high temperatures were limited, the extrapolation produces results which are accurate only to within about 1 mol %. Nevertheless, the coordinates of the intersection point, namely 16 % Ga_2S_3 and 818 °C, represent the best estimate of the eutectoid composition and temperature currently available. A similar extrapolation applied to the phase boundaries at the sphalerite-rich and thiogallate-rich ends of the phase diagram places the compositions of the reactant phases as ~9 and ~40 mol % Ga_2S_3, respectively. The phase boundaries indicated by the shaded curves in Fig. 1 are consistent with those determined quantitatively.

We note that the solubility of ZnS increases with increasing temperature. Consequently, both eutectoid decomposition and precipitation hardening can be potentially utilized to manipulate the mechanical properties of ZnS-Ga_2S_3 ceramics, as discussed by Zhang et al.[5]

SUMMARY

The ZnS-Ga_2S_3 phase diagram, from 700 to 900 °C and to 50 mol % Ga_2S_3, was determined using x-ray diffraction techniques from samples prepared via the solid-state reaction of powders. The wurtzite (W), sphalerite (S) and tetragonal thiogallate (T) phases all exist over a considerable range of stoichiometry. There is a eutectoid reaction at 818 °C in which W (16 mol %) decomposes to S (9 %) + T (40 %). The solubility of Ga_2S_3 in ZnS increases with increasing temperature below the eutectoid temperature.

ACKNOWLEDGEMENT

Financial support for this research was provided by the Office of Naval Research under Contract No. N00014-87-K-0531.

REFERENCES

1. E. W. Kruse III and M. E. Fine, "Precipitation Strengthening of MgO by $MgFe_2O_4$", *J. Am. Ceram. Soc.*, **55**, 32-37 (1972).

2. V. D. Krstic and P. S. Nicholson, "Fracture of LiF-MgF_2 Precipitated Composites", *J. Am. Ceram. Soc.*, **64**, 644-48 (1981).

3. A. G. Evans and R. M. Cannon, "Toughening of Brittle Solids by Martensitic Transformations", *Acta Metall.*, **34**, 761-800 (1986).

4. W. W. Chen, J. M. Zhang, A. J. Ardell and B. Dunn, "Solid-State Phase Equilibria in the ZnS-CdS System", *Mater. Res. Bull.*, **23**, 1667-73 (1988).

5. J. M. Zhang, W. W. Chen, B. Dunn and A. J. Ardell, "Phase Diagram Studies of ZnS Systems", *Ceramics and Inorganic Crystals for Optics, Electro-Optics, and Nonlinear Conversion*, R. W. Schwartz, Editor, Proc. SPIE **968**, pp. 35-40 (1988).

6. A. S. Gates and J. G. Edwards, "Vapor Pressures, Vapor Compositions, and Thermodynamics of the $ZnGa_2S_4$-$ZnGa_8S_{13}$ System by the Simultaneous Knudson and Dynamic Torsion-Effusion Method.", *J. Phys. Chem.*, **82**, 2789-97 (1978).

7. A. Yu. Malevskii, "Ranges of Isomorphic Replacement in the System ZnS-Ga_2S_3", in Eksp. Issled. Obl. Geokhim. Kristallogr. Redk. Elem., Akad. Nauk SSSR, Inst. Mineral., Geokhim. Kristallogr. Redk. Elem., 12-20 (1967).

8. P. Wu, X.-C. He, K. Dwight and A. Wold, "Growth and Characterization of Zinc and Cadmium Thiogallate", *Mater. Res. Bull.*, **23**, 1605-09 (1988).

9. G. B. Carpenter, P. Wu, Y.-M. Gao and A. Wold, "Redetermination of Crystal Structure of Zinc Thiogallate", to be published, *Mater. Res. Bull.*

10. D. L. Chess, C. A. Chess and W. B. White, "Physical Properties of Ternary Sulfide Ceramics", *Mater. Res. Bull.*, **19**, 1551-58, (1984).

11. B. D. Cullity, *Elements of X-ray Diffraction*, 2nd edition, Addison-Wesley, Reading, MA, p. 369 (1978).

12. H. P. Klug and L. E. Alexander, *X-Ray Diffraction Procedures*, John Wiley & Sons, New York, NY, p. 410 (1954).

13. W. Dollase, unpublished research.

Table I. Solid-state reaction conditions.

T (°C)	Time (hr)
700	1700
750	550
800	1400
850	910
900	385

FIGURE CAPTIONS

Fig. 1 Phase map of the ZnS-Ga_2S_3 system to 50 mol %. The shaded regions show the most likely locations of the phase boundaries. The open circles indicate the presence of sphalerite (S), the open squares the presence of wurtzite (W) and the filled circles the presence of thiogallate (T).

Fig. 2 Illustrating the use of the disappearing-phase method to determine the boundaries between: (a) Wurtzite and sphalerite at 850 °C; (b) Wurtzite and thiogallate at 900 °C.

Fig. 3 Illustrating the use of the parametric method to determine: (a) The S/(S + T) solvus at 700 and 750 °C; (b) The T/(S + T) solvus at 700 and 800 °C. In (b), **a** refers to $\mathbf{a}_t$.

Fig. 4 The ZnS-Ga_2S_3 phase diagram to 50 mol %, from 700 to 900 °C.

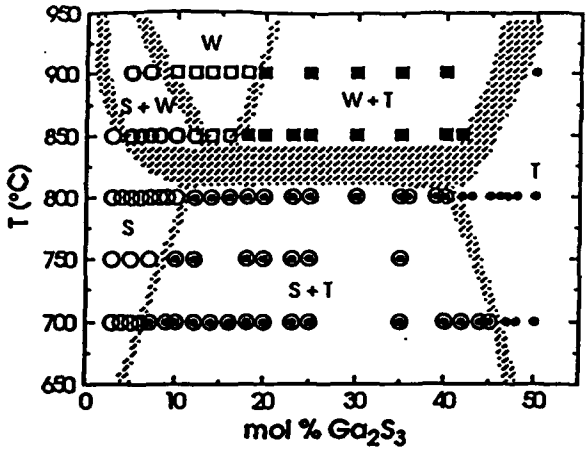

Fig. 1 Phase map of the ZnS-Ga_2S_3 system to 50 mol %. The shaded regions show the most likely locations of the phase boundaries. The open circles indicate the presence of sphalerite (S), the open squares the presence of wurtzite (W) and the filled circles the presence of thiogallate (T).

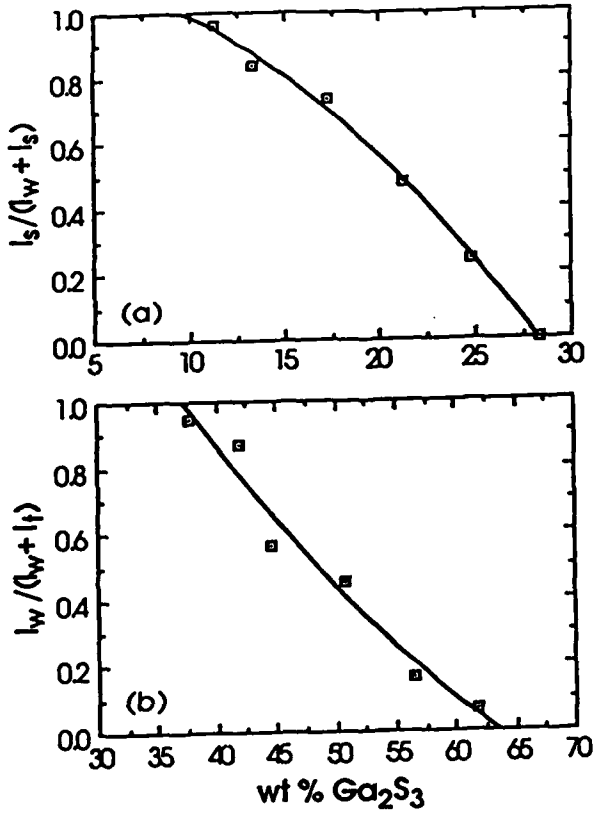

Fig. 2 Illustrating the use of the disappearing-phase method to determine the boundaries between: (a) Wurtzite and sphalerite at 850 °C; (b) Wurtzite and thiogallate at 900 °C.

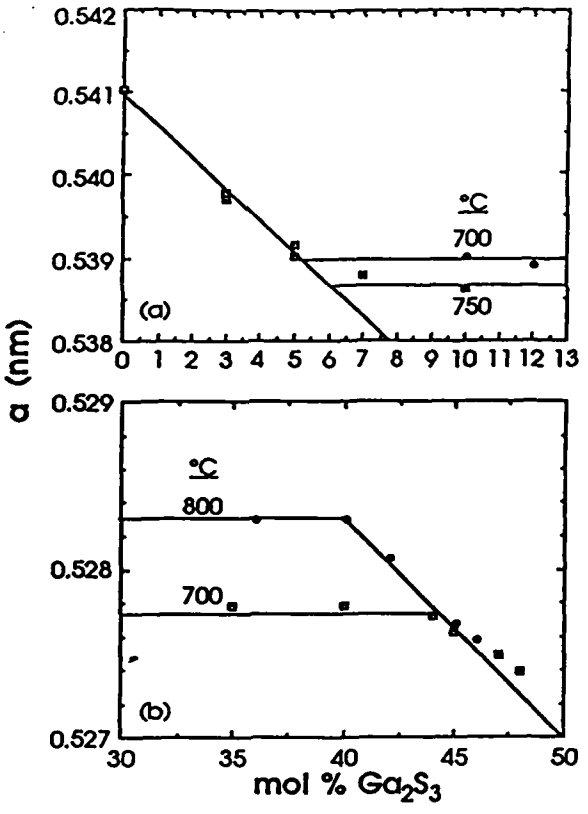

Fig. 3 Illustrating the use of the parametric method to determine: (a) The S/(S + T) solvus at 700 and 750 °C; (b) The T/(S + T) solvus at 700 and 800 °C. In (b), a refers to a_t.

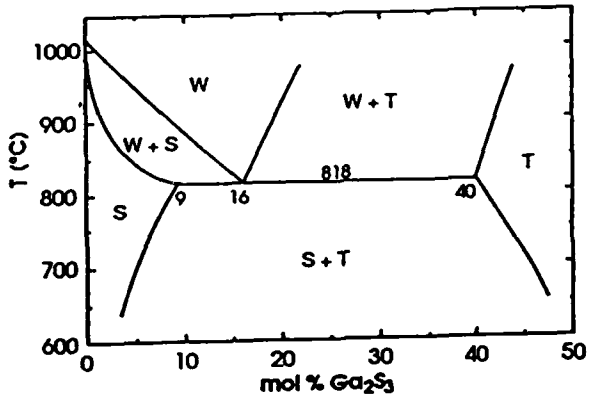

Fig. 4 The ZnS-Ga_2S_3 phase diagram to 50 mol %, from 700 to 900 °C.